Identification of environmental factors controlling wine quality: A case study in Saint-Emilion Grand Cru appellation, France

Etienne Fayolle, Stéphane Follain, Philippe Marchal, Philippe Chéry, François Colin

Science of the Total Environment 694 (2019) 133718

Contents lists available at ScienceDirect

Science of the Total Environment

journal homepage: www.elsevier.com/locate/scitotenv

Identification of environmental factors controlling wine quality: A case study in Saint-Emilion Grand Cru appellation, France

Etienne Fayolle [a,b], Stéphane Follain [a,c,*], Philippe Marchal [b], Philippe Chéry [d], François Colin [a]

[a] UMR LISAH, Univ. Montpellier, Montpellier SupAgro, Montpellier, France
[b] Antoine Moueix Propriétés, Saint-Emilion, France
[c] Agroécologie – AgroSup Dijon, INRA, Univ. Bourgogne, Univ. Bourgogne Franche-Comté, Dijon, France
[d] Bordeaux Sciences Agro, EA4592 G&E, Bordeaux, France

HIGHLIGHTS

- The winter water table rise had a major impact on the root pattern.
- The water table dynamics modified the ability of the vine to water and nutrient uptake.
- Soil map and wine quality ranks map had a good accordance.
- Best wine is observed for moderate water deficit and no-limited nutrient conditions.

GRAPHICAL ABSTRACT

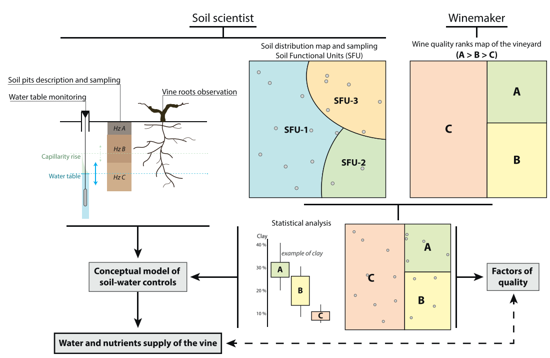

ARTICLE INFO

Article history:
Received 22 April 2019
Received in revised form 31 July 2019
Accepted 31 July 2019
Available online 01 August 2019

Editor: Jay Gan

Keywords:
Soil
Vine
Vineyard
Terroir
Water table
Water and nutrients supply

ABSTRACT

Soil is a key component of the terroir concept for wine production. Indeed, the soil provides water and nutrients to the vine plants depending on its properties and environmental conditions. A part of the complexity in the production of high-quality wines is the adaptation of the winegrowing practices to soil conditions variability in space and time. Then, a deep understanding of the environmental conditions that modulate soil-plant system functioning and control the production of quality wine is crucial for future global change adaptation. This study aimed to identify environmental factors controlling red wine quality by merging both winemaker and scientist knowledge. This work was performed on a vineyard in Saint-Emilion Grand Cru appellation, France. First, we conducted field investigations for micro-terroir scale soil mapping in 2017, based on pedological prospections (pits and auger borings) and both water table levels and main meteorological parameters monitoring (from November 2017 to November 2018). Additionally, we collected for each vineyard plot the corresponding wine quality rank established each year since 2012 and based on wine tasting sessions supervised by the winemakers. Subsequently we investigated both nutrients and water availability for the vine. This was achieved through correlative analysis using soil description, roots observation and water table level, stratified according to both soil functional units and wine quality ranks maps. Results show that the water table dynamic and the soil texture have a major impact on the root pattern of vines. Our study suggests that explanatory factors for wine quality are interactions between soil-water and roots during vine crop season. Here, best soils for fine wines could be observed for both non-severe water deficit and no-limited nutrient conditions.

* Corresponding author at: AgroSup Dijon, 26 Bd Docteur Petitjean, BP 87999, 21079 Dijon Cedex, France.
E-mail address: stephane.follain@agrosupdijon.fr (S. Follain).

https://doi.org/10.1016/j.scitotenv.2019.133718

1. Introduction

Soil is a key component for wine production (White, 2003) and a main component of the terroir concept (Deloire et al., 2005; Van Leeuwen et al., 2004; Vaudour, 2002), even if the relationships between wine sensory attributes and geological or soil characteristics have been widely discussed (Maltman, 2008; Matthews, 2016). The basic relationship between wine and soil is based on the water and nutrient requirements of the vine plants (White, 2003). Soil variability in space and time and soil–climate interactions are the main drivers for terroir differentiation on a large spatial scale (Costantini et al., 2018, 2015; Garcia et al., 2018; Priori et al., 2019; Rodrigo-Comino, 2018; Vaudour, 2002). For finer spatial resolution, human effects are essential; over time, human-landscape structure and short-term practices can significantly modify pedological properties and variability on a field plot scale (Costantini et al., 2015) while affecting both water and carbon dynamic and thus soil erosion (Costantini et al., 2018, 2015; Garcia et al., 2018).

Soil characteristics, such as pH and nutrient supply, are mainly derived from geological rocks and are critical for vine growth and wine quality (Kodur, 2011; Retallack and Burns, 2016). The relationship between the soil nutrient status and wine quality varies depending on plant physiology and environmental interactions (Blotevogel et al., 2019; Garcia et al., 2001; Mackenzie and Christy, 2005). The addition of water dynamics to the physical properties of soil modulates water availability and vine root architecture, and subsequently, water and nutrient composition (Morlat and Bodin, 2006). This complexity of nutrient studies explains why a majority of studies on soil–wine interactions has investigated the status of water relationships. The main finding of such studies is that red wine grape quality is often associated with a mild water deficit (Bonfante et al., 2011; Brillante et al., 2016; Costantini et al., 2013; Deloire et al., 2005; Dry, 2016; Marciniak et al., 2013).

A part of the complexity for winegrowers and winemakers in the production of high-quality wines is the adaptation of their practices to terroir conditions or specificities in space and time. In future, the adaptability of winegrower practices will be a key issue for the adaptation of wine appellations to climate-related changes as predicted by projections of future climate change (IPCC, 2014). Climate variations and specificities are already recognised as the main factors controlling grape maturation, aroma, and coloration (Baciocco et al., 2014; Camps and Ramos, 2012; Jones and Davis, 2000; Tonietto and Carbonneau, 2004; Van Leeuwen et al., 2004), which are a part of wine identity. However, the success of this adaptability presumes a fine understanding of soil, climate, and vine interactions.

Knowledge of the environmental factors that modulate soil functioning and control the production of quality wine is lacking, which is a potential deficiency for future adaptability (Hannah et al., 2013). Generally, nutrient-focused studies are driven on superficial topsoil horizons, whereas vine root systems prospect over a large volumes both in organo-mineral and mineral soil horizons (Archer and Saayman, 2018). Additionally, water-focused studies consider water availability at the soil pedon scale or for theoretical soil conditions without integrating in- and out-flow boundary conditions or considering water-table level dynamics. For these reasons, we propose that future studies should couple investigations of both nutrient and water supply based on fine description and analysis of the pedon, from the topsoil to the maximum rooting depth as proposed by Costantini and Bucelli (2014).

The aim of this study was to identify environmental factors controlling both nutrient and water supply to the vine plant and then affecting red wine quality. First, we performed high-resolution pedological investigations integrating physical–chemical properties, vine root observations, and water table depth dynamics on a Saint-Emilion Grand Cru vineyard. Then, we analysed the results based on stratification from a wine quality map elaborated by the estate winemaker. Finally, we discussed and proposed a conceptual model for water and nutrient availability by considering the whole soil profile depth and integrating the boundary conditions induced by different environmental conditions.

2. Material & methods

2.1. Study site

The study was carried out in the Saint-Emilion Grand Cru appellation area (Fig. 1), a part of the largest Bordeaux winegrowing area in the southwest of France. The Saint-Emilion Grand Cru appellation (Appellation d'Origine Controlée –AOC) extends over nine village territories containing 5500 ha of vines (Ministère de l'Agriculture et de l'Alimentation, 2017a). An official decree allows five grape varieties: Merlot (60%), Cabernet franc (30%), Cabernet sauvignon (10%), Malbec, and Carmenere (Ministère de l'Agriculture et de l'Alimentation, 2017b). Within this appellation area, the study site is the vineyard of the Château Capet-Guillier, located in Saint-Hippolyte village territory (44°52′27″ N; 0°7′9″ W), 5 km east of the city of Saint-Emilion. The Château Capet-Guillier is a vineyard about 13 ha in production, which produces red wine based on three grape varieties: Merlot (85%), Cabernet franc (5%), and Malbec (10%). Field plots have an average surface of 1 ha ($\pm$0.57 ha standard deviation) and are located on an exposition south-facing foot slope (Fig. 3).

The main vine variety is Merlot N associated to two rootstocks *i.e.* 101-14 Millardet et de Grasset (101-14 MGt) and Riparia Gloire de Montpellier. The average planting density on the study site is of 6745 plants per hectare with a row spacing of 1.45 m. Inter-row space are cover cropped and integrate service crops (*Avena sativa*, *Secale cereal* and *Vicia sativa*). Typical soil tillage operations are (i) deep tillage such as deep mouldboard ploughing at depths of about 0.5 m at pre-planting time, (ii) surface tillage operations to a depth of 0.05–0.10 m such as chiselling throughout the vineyard's life cycle and (iii) mechanical weeding at depth of 0.2 m using ripper tools after the grape harvest, in order to prepare next service crop sowing in November. A yearly maintenance fertilization based on organic fertilizers was realized by the winegrower. Depending on each vine plot needs, applied quantity could vary from 300 to 400 $kg.ha^{-1}$.

The geology of the Saint-Emilion appellation (1:50,000) has been mapped by the French Geological and Mining Research Agency (Dubreuilh, 1995). This map points out a limestone formation (Asteria limestone) which is overlaid by tertiary sediments and constitutes the plateau relief. This plateau has been shaped by three rivers, Dordogne, Isle, and Barbanne, which flow within the tertiary sediments. Deeper geological layers, beneath the Asteria limestone, include the limestone and clay of Castillon, which constitute the upper part of the slope system. The lower part of the slope system constitutes the Fronsadais Molasses formation (a calcareous formation composed of sand, silt, and clay) affected by colluvium in the lowest part. Southward lies an alluvial plain, formed by the Dordogne river during the Quaternary period. Associated alluvial sediments are mainly sands with sparse gravel terraces (Dubreuilh, 1995). Field plots of the Château Capet-Guillier are located on different geological formations: from tertiary calcareous formations on the slope system to Quaternary sandy alluvium on the plain system.

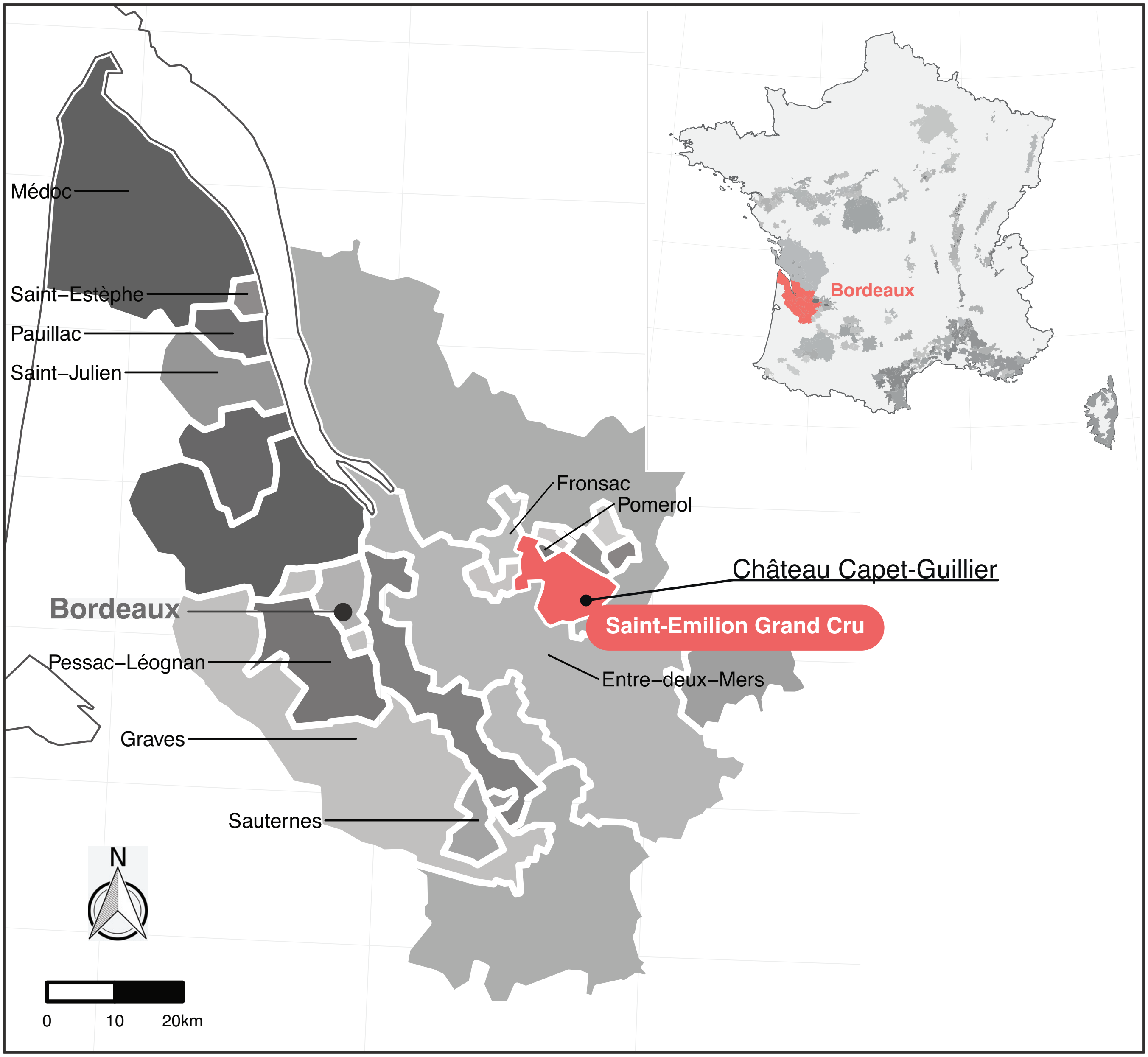

Fig. 1. Location of the study site: Château Capet-Guillier in Saint-Emilion Grand Cru appellation.

A soil map of the Saint-Emilion appellation (1:25,000) was produced by Van Leeuwen (1989). The map proposed the categorisation of soil diversity based on geomorphic zones. The soil classification used by Van Leeuwen was transformed into WRB classification (IUSS Working Group WRB, 2015). The map with new soil classification defines two geomorphic zones on the Château Capet-Guillier vineyard perimeter: i) the slope system with Calcaric Cambisols with fine silt soil texture, and ii) the plain system with Calcaric Cambisol, Gleyic Luvisol (arenic), and Epicalcaric Stagnosol clayic (IUSS Working Group WRB, 2015).

The climate of the area is temperate oceanic, classified as *Cfb* in the Köppen classification (Peel et al., 2007). According to data records for 1981–2010 from the Mérignac meteorological station (44°49′48″ N; 0°41′2″ E) of the French National Meteorological Service (Météo France), the winters are mild and rainy, and the summers are moderately warm and dry with mean rainfall of 944 mm per year and a mean annual temperature of 13.8 °C. The inter-annual weather variability is relatively high and implies a strong vintage effect on the wines (Bois et al., 2008). An ombrometric diagram (available in Supplementary data) shows that rainfall is distributed throughout the year with no significant dry period in summer.

2.2. Data collection

2.2.1. Soil survey

A soil survey (sampling design available in Supplementary data) was carried out to obtain a high-resolution soil map (1:2500). First, a base map was produced by soil auger up to 1.2 m deep, with a spatial density of six augers per hectare. Each auger boring was described and sampled according to the Food and Agriculture Organization of United Nations (FAO) rules for soil descriptions (Jahn et al., 2006). Then, the soil horizon and soil types, identified during the field study, were classified according to the World Reference Base (IUSS Working Group WRB, 2015). To refine this base map, three additional samplings were included: i) a topsoil sampling of organo-mineral horizons (A-horizons), from the soil surface to 0.20 m soil depth with a spatial density of 10 samples per hectare; ii) four mechanical cores, which were drilled, described, and sampled to a maximum depth of 4.50 m, and two were transformed as permanent piezometers and used to monitor the water table level; and iii) 15 pedological pits were dug to describe the main morphological traits of soil and to accurately sample soil volume in each soil horizon type. The average depth of the pits was 1.60 m. Regardless of the soil sampling strategy, all collected samples were air-dried (48 h at 40 °C) and passed through a 2.0 mm sieve for prior determination of classical chemical parameters. The bulk density of the different horizons was measured by sampling the soil core (5 cm high, 8 cm in diameter). The abundance and size of roots and particular root orientation were described according the methodology given by the guideline of the FAO (Jahn et al., 2006).

2.2.2. Climate data and meteorological index

Two different meteorological data series were used in this study. The first series was from the regional Mérignac meteorological station (44°49′48″ N; 0°41′24″ E) of the French National Meteorological Service (*Météo France*). This series provides daily data from 1920 onwards. The second series was from a local meteorological station on the study site (Davis® model). This station was installed in the alluvial plain in April 2017 and records hourly data. It allows classical meteorological parameters to be recorded and calculated, such as rainfall, temperature, humidity (air and soil), winds, and global radiation. The Penman–Monteith reference evapotranspiration (ET_0) was calculated using the equation described by Allen et al. (1998).

To analyse the climate characteristics in relation to vine production, classic climate indices commonly used in vine sciences were utilised (Tonietto and Carbonneau, 2004): the Heliothermal Index (HI), the cool night index (CNI), and the dryness index (DI).

The HI, described by Huglin, is a bioclimatic heat index developed for vineyards. As the Winkler index, it is a heat sum indicator, corrected by a day-length coefficient related to the geographical latitude. The index calculation uses both the daily mean temperature (°C) and the daily maximum temperature (°C), reduced to a baseline temperature (10 °C for vine) (Huglin, 1978). We calculated the daily HI from April to September with a latitude coefficient $d = 1.04$ following the data and equation (Eq. (1)) given by Tonietto and Carbonneau (2004). T_m is the mean air temperature (°C), and T_x is the maximum air temperature (°C).

$$\mathrm{HI} = \sum_{01.04}^{30.09} \frac{(\mathrm{T_m} - 10) + (\mathrm{T_x} - 10)}{2}.\mathrm{d} \tag{1}$$

The CNI considers the mean minimum night temperatures (°C) during the month before the harvest when the berries are ripening (Eq. (2)). The aim of this index is to evaluate the qualitative potential of wine-growing regions, especially in relation to secondary metabolites in wine. In the northern hemisphere, September was selected to calculate the CNI (Tonietto and Carbonneau, 2004).

$$CNI = \text{average minimum air temperatures in September (°C)} \tag{2}$$

The DI was also calculated following the method given by Tonietto and Carbonneau (2004) (Eqs. (3a), (3b), (3c)). This index evaluates the climatic demand for a standard vineyard without runoff and bare soil evaporation. Similar to the HI, the DI was calculated from April to September. First, E_S and T_V were calculated monthly according to the calculation described by Tonietto and Carbonneau (2004): (i) E_S is the direct evaporation from soil (mm) for the considered duration (Eq. (3a)), where ET_0 is the monthly total reference evapotranspiration using Penman method (Penman, 1948), N is the number of day in the month, k is related to the vine architecture and changes with the increase of the leaf area during the season: k = 0.1 in April, k = 0.3 in May and k = 0.5 from June to September (in the northern hemisphere), and JP_m is calculated by using the total rainfall of the month in mm divided by 5 (this is an estimation of the number of day of effective evaporation, so it should be ≤N). (ii) T_V is the potential transpiration in the vineyard (mm) for the considered duration (Eq. (3b)). The DI is based on a water balance calculation (Eq. (3c)), where W_0 is a theoretical initial water value (200 mm), P is the total amount of precipitation (mm) for the considered duration.

$$E_S = \frac{ET_0}{N}.(1-k).JP_m$$

$$T_V = ET_0.\mathrm{k}$$

$$DI = W_0 + \sum_{01.04}^{30.09} P - E_s - T_V \tag{3c}$$

2.2.3. Groundwater monitoring

Two monitored piezometers (4.50 m in depth) were installed in 2017, one in each geomorphological sector (Fig. 3). The first was located in the alluvium plain sector (P1, 12.9 m a.s.l.) and the second was located in the foothill sector (P3, 16.8 m a.s.l.). Both were supplied with a pressure probe and data-logger (*Rugged TROLL 100*). Data-logging monitoring began in November 2017 with two measurements per hour. Barometric correction for piezometers was performed with barometric data from the installed meteorological station (c.f. 2.2.2).

2.2.4. Vine available water estimation

Considering the influence of water supply on berry quality, we estimated the vine available water capacity (AWC), based on the soil properties determined in soil pits (Table 1). The calculations were performed using pedotransfer functions by Bruand et al. (2004), which estimate the humidity characteristics of each horizon type (A- and B-horizons) based on measured soil texture and soil bulk density (c.f. results 3.3 Soil descriptions, Table 1). Then, AWC was estimated by integrating different root zone conditions: (i) C-AWC, AWC calculated at the conventional depth of 1.0 m, and (ii) P-AWC, potential AWC calculated according to the maximum potential rooting zone observed in the soil pits. In addition, considering the limitations associated with AWC calculation (Lacape et al., 1998; Pellegrino et al., 2004; Ratliff et al., 1983), we also calculated the total transpirable soil water (TTSW) according to the formula (Eq. (4)) developed by Bertrand et al. (2018), which considers the depth of the maximum root density and ability of the roots to extract water at a water potential different from the theoretical wilting point (Pellegrino et al., 2004; Ratliff et al., 1983).

$$TTSW = \int_0^{Erd} (\theta_{fc}(z) - \theta_{minus}(z))dz \tag{4}$$

With Erd the effective rooting depth; $\theta_{fc}(z)$ the field capacity humidity for each soil horizon estimated using pedotransfer functions by Bruand et al. (2004) according to the soil texture and bulk density; $\theta_{minus}(z)$ the minimum soil humidity threshold for each horizon under which the vine cannot extract water. The values of θ_{minus} depend on soil and plant characteristics. The values we used for vine have been estimated following the BISWAT parameterization protocol as suggested in Bertrand et al. (2018): the authors provide a simple model using two parameters α and β to calculate θ_{minus} from $\theta_{wilting\ point}$: α is the plant parameter in relation with the anisohydric character of the vine, the value we used for the vine is 1.4 according to the humidity measurements presented by Pellegrino et al. (2004); β corresponding to the depth from which the root density begins to decrease. According to this model, θ_{minus} is calculated as follows:

(i) from surface to depth β: $\theta_{minus} = \alpha.\ \theta_{wiltingpoint}$
(ii) from depth β to depth *Erd* (effective rooting depth): θ_{minus} linearly increase until $\theta_{field\ capacity}$

$\theta_{field\ capacity}$ and $\theta_{wilting\ point}$ are the same characteristic humidities we used in AWC calculation (using pedotransfer functions by Bruand et al. (2004)).

2.2.5. Wine quality survey

Several studies focusing on the terroir effect have assessed grape quality using measurements of vines or berries (Dry and Loveys, 1998; Vaudour, 2002; de Andrés-de Prado et al., 2007; Van Leeuwen et al., 2009; Van Leeuwen, 2010; Bonfante et al., 2011; Costantini and Bucelli, 2014). In the present study, we integrated the wine quality ranking by the winemaker. This was motivated by several factors: (i) good berry quality is not sufficient to imply a high wine quality; (ii) considering that bottled wine quality is potentially biased, it is traditional practice in the Bordeaux region to blend different grape varieties and plots of a vineyard into a single vintage; (iii) consideration of wine quality allows a human factor to be integrated into the analysis; (iv) wine quality ranks map represents the real integration in space and time of many years of production, and the subsequent integration of experience from several vintages.

In Saint-Emilion, the predominant variety is Merlot assembled with Cabernet franc. To improve the final wine quality, the current process is to separate grapes during the harvest, on a plot or subplot scale (micro terroir zoning). Afterwards, it is possible to use numerous and small winemaking tanks to separate fermentation. At the end of the separation process (from field to wine), the winemaker can identify the quality of each (sub)plot and choose the best blend before the bottling step. Based on these practices, the winemaker uses a plot-by-plot approach to assess the quality and potential of his vineyard.

At Château Capet-Guillier, the grape from each plot are vinified in separate tanks. After vinification, the wine batches are tasted by three oenologists who attribute a quality rank: from A (the best) to C (the worst). Markers for quality ranking by oenologists are: (i) length in mouth, (ii) tightness/balance (acidity and alcohol), (iii) tannins intensity, (iv) color, (v) maturity and smoothness of tannins, (vi) aromatic complexity. Each marker is rated from 1 to 5, and final wine quality rank (A to C) is attributed with the highest quality rank if minimum rate for all markers is reached (Fig. 4).

2.3. Statistics and data analysis

Statistical analyses were performed using the R software (R Core Team, 2014). Geographical data were processed, and the soil map was created using the software QGIS3 (QGIS Development Team, 2019).

3. Results

3.1. Climate data and index

The main meteorological statistics and meteorological indices (HI, CNI, and DI) are summarised in Supplementary data. Regional meteorological data, recorded at Mérignac station for 1987–2017, revealed a mean annual rainfall of 912 mm with a standard deviation of 180 mm. The amount of rainfall in 2017 and 2018, as recorded by the local station, was 749 and 905 mm, respectively. The mean annual temperature at Mérignac station was 13.7 °C with an inter-annual variability of 0.6 °C (standard deviation), whereas the annual values were 13.6 °C (2017) and 14.0 °C (2018). Regional recordings were associated with a mean ET_0 value of 944 mm (standard deviation 32 mm), whereas local measurements for 2017 and 2018 varied from 811 to 826 mm. The meteorological indices, calculated based on the long-term series, were 2101 °C for HI, 13.2 °C for CNI, and 107.2 mm for DI. Based on the HI value, the regional climate was classified as *temperate* and *warm temperate*. Growing degree days (GDD) were also calculated with a base temperature of 10 °C (Winkler et al., 1974; Bonfante et al., 2018). These results class the area in Region II: early and mid-season table wine varieties will produce good quality wines according to the Winkler Index scale. For the CNI and DI indices, according to the classification proposed by Tonietto and Carbonneau (2004) (Supplementary data), the Bordeaux climate was defined as *temperate and sub-humid with cool nights*. The same indices calculated on the study site, showed that our vineyard conditions were slightly higher for HI index, cooler for CNI, and wetter for DI.

3.2. Water table level dynamics

The upper part of Fig. 2 presents the daily rainfall and associated cumulative rainfall curve (ribbon) from November 2017 to November 2018, measured at the local meteorological station. The lower part of Fig. 2 presents daily water table depths measured at the two piezometer locations; piezometer P1 (12.9 m a.s.l.) located on the plain, and piezometer P3 (16.8 m a.s.l.) located in the foothill (Fig. 3). Because of a dry summer in 2017, the end of 2017 was characterised by low water table levels on both piezometers, between 10.9 and 11.8 m a.s.l. Subsequent rainfall events around the 10th of December (100 mm in 9 days) were responsible for the first significant increase in the water table (0.2 m), similar in quantity for both piezometers, although more gradual for P2. Then, the transition from 2017 to 2018 was characterised by high amounts of rainfall: >100 mm from the 25th of December to the 7th of January. In relation to this amount of rainfall, variation in the water table level in both piezometers was increased by about 1.3 m. At the end of January, the water level of P1 reached a plateau with a minimum depth from soil surface topography to the water table level of 0.5 m, which was observed on the 1st of April. The same trend for rising water levels was observed for piezometer P3; however, for this last position, the overall increase was higher than that observed for P1 and no plateau was observed prior to the minimum depth (1.5 m), which occurred during the same period, *i.e.* the beginning of April. From April to November, there was a general trend for a two-step decrease, clearly separated by rainfall events that occurred in June. After mid-June, the decrease was more pronounced while the precipitation rate was <60 mm per month. On the 1st of November, both piezometers reached their baseline levels: 2.75 and 5.78 m below ground for P1 and P3, respectively.

3.3. Soil descriptions

Fig. 3 shows a soil map of the study site, based on field investigations. The area (13.2 ha) is composed of 13 soil units (SU) (IUSS Working Group WRB, 2015) distributed in two main soil types: (i) Cambisols with clayey-dominated soil textures on hillslope, clearly linked to underlying calcareous geological formations (SU-11 to 15) and (ii) Fluvisols from sandy to clayey soil texture in the plain area developed within old alluvial deposits (SU-1 to 8). The high sampling density allowed us to identify an intermediate domain on the eastern part of the plain area (SU-6, 7, and 8) where carbonated colluvium originated from the slope overlaying pre-existing Fluvisol. Waterlogging was observed for most SUs in the plain area, but at different depths. The west part of the plain (SU 1 to 5) was marked by deep waterlogging as the texture of the horizons became finer. The east part (SU 6 to 8) was topographically lower, hence waterlogging appeared in the shallower horizon.

Based on the map, we defined three soil domains, termed soil functional units (SFU) (Fig. 3): (i) SFU-1 for Fluvisol in the western part of the plain area, (ii) SFU-2 for Fluvisol in the eastern part of the plain overlaid by colluvium, and (iii) SFU-3 for Cambisol on the hillside. From a pedological perspective, each SFU was associated with a pedological

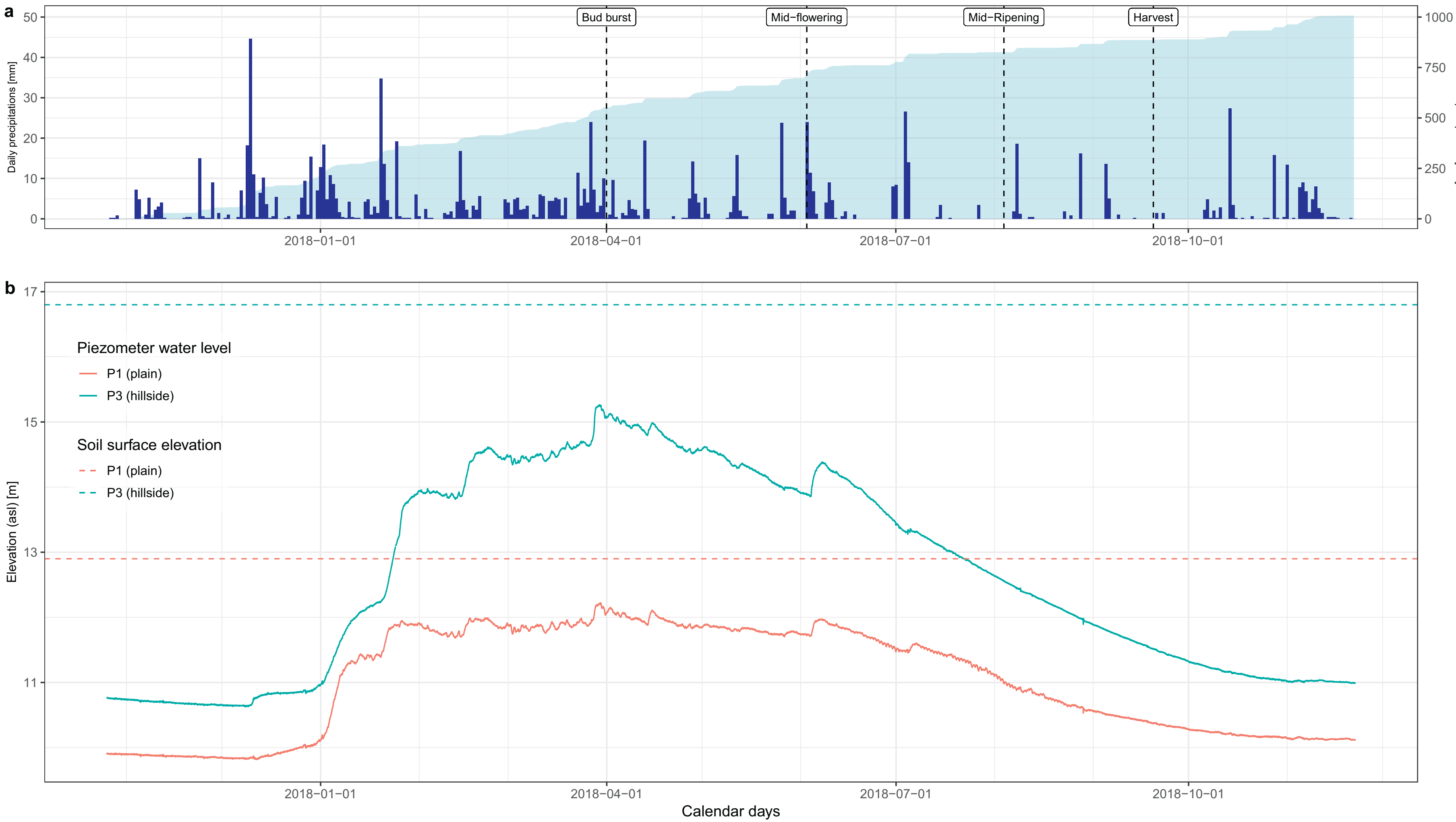

Fig. 2. (a) Groundwater monitoring from November 2017 to November 2018. Daily and cumulative rainfall; (b) piezometric levels of P1 (12.9 m a.s.l.) and P3 (16.8 m a.s.l.).

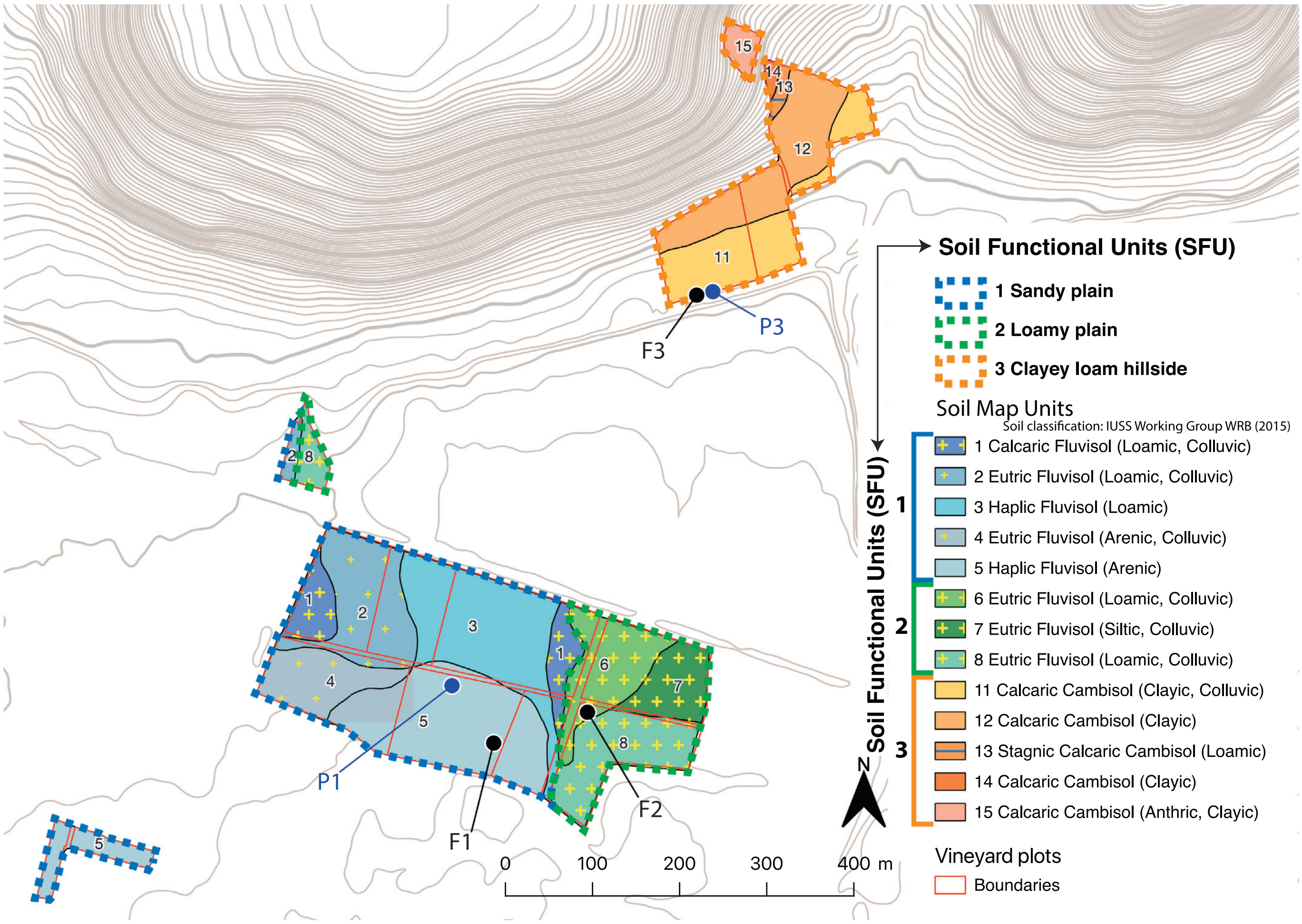

Fig. 3. Pedological map of Château Capet-Guillier. Localisation of the pits (black) and the piezometers (blue). (For interpretation of the references to color in this figure legend, the reader is referred to the web version of this article.)

trench (F1 for SFU-1, F2 for SFU-2, and F3 for SFU-3), whose descriptions and properties are summarised in Table 1.

F1 has a deep soil profile (over 1.2 m) with sandy-dominated soil textures, except for deep soil horizons (>0.92 m), where the clay fraction increases significantly. The overall soil profile is composed of several soil horizons with topsoil organo-mineral horizons (A-horizon) within the first 0.36 m. A low organic carbon content characterised these A-horizons (0.45%) with a pH value of 7.1 and a very low cation exchange capacity (CEC; 2.9 cmol+/kg). With depth, soil horizonation evolved through mineral horizons (B-horizons) that were characterised by similar soil properties, except the decreasing CEC value in relation to decreasing total organic carbon (TOC) content. We noted that deeper

Table 1
Description and analysis of the soil pits (F1, F2 and F3).

Pit	Hz name [FAO]	Depth [cm]	CLAY [%]	SILT [%]	SAND [%]	TOC [%]	N total [‰]	C/N [−]	CEC [cmol +/kg]	CaO [mg/kg]	MgO [mg/kg]	K2O [mg/kg]	Na2O [mg/kg]	pH [−]	Total $CaCO_3$ [%]	Bulk density [g/cm$_3$]
F1: Haplic Fluvisol (Arenic)	Ap1	0–12	5.8	8.0	86.1	0.41	0.40	10.2	3.6	992	57	96	1.5	7.3	<0.5	1.44
	Ap2	12–36	5.6	9.5	84.9	0.47	0.50	9.3	2.5	972	59	63	6.0	7.0	<0.5	1.53
	B	36–54	5.4	7.9	86.7	0.17	0.20	8.7	1.4	796	45	74	7.0	7.8	<0.5	1.51
	Bw(o)	54–74	13.3	7.5	79.2	0.17	0.20	8.7	2.4	804	79	70	5.0	7.2	<0.5	1.70
	Bo	74–92	6.9	6.8	86.3	0.06	0.10	5.8	1.0	332	38	47	1.5	7.2	<0.5	1.60
	Bwg	92–125	21.8	16.5	61.8	0.06	0.20	2.9	10.5	2658	248	139	15.0	7.2	<0.5	1.67
F2: Eutric Fluvisol (Loamic, Colluvic)	Apk1	0–15	25.7	23.5	50.8	1.16	2.00	5.8	13.6	9326	298	209	12.0	8.2	3.5	1.31
	Apk2	15–32	26.9	25.2	47.9	0.58	0.58	10.0	11.5	10,371	339	97	13.0	8.4	9	1.66
	Bwk	32–60	24.0	15.3	60.7	0.29	0.31	9.4	10.3	9036	363	60	13.0	8.5	2.9	1.70
	Bwko1	60–105	23.0	13.7	63.4	0.23	0.25	9.3	10.8	8969	493	69	19.0	8.5	2.4	1.62
	Bwko2	105–150	15.5	13.1	71.3	0.12	0.16	7.3	5.1	9365	310	36	11.0	8.7	19.5	1.55
	Cg	150–160	1.7	6.1	92.3	0.06	0.05	11.6	3.6	2235	119	34	6.0	8.6	<0.5	1.60
F3: Calcaric Cambisol (Clayic, Colluvic)	Apk	0–20	28.5	47.4	24.2	1.69	1.90	8.9	11.6	10,658	340	297	12.0	7.9	29.7	1.17
	Bwk1	20–70	31.1	51.3	17.6	0.41	0.64	6.3	10.8	10,576	461	227	9.0	8.3	39.5	1.61
	Bwk2	70–130	36.0	55.5	8.4	0.47	0.70	6.6	12.0	10,662	548	205	142.0	8.2	32.2	1.57
	Ck	130–160	36.0	48.9	15.1	0.47	0.69	6.7	12.7	10,842	561	157	16.0	8.1	22.1	1.57

soil horizons (>0.92 m) with a high clay fraction (21.8%) also presented the highest CEC value (10.5 cmol+/kg). When describing the soil, we observed waterlogged soil horizons (Bw-horizon) with waterlogged features starting at 0.54 m, whose density increased in the deepest soil horizons and evolved from a status of oxidation to reduction. This observation of waterlogging was corroborated by vine root architecture, as the main root fraction decreased after the first 0.74 m of soil, and the lateral development of roots was important.

The F2 soil profile was also deep, with significant differences compared with F1. Here, the soil texture was always dominated by the sand fraction; however, the topsoil horizons presented significant clay (25.7%) and silt (23.5%) fractions. With soil depth, there was an increase in the sandy fraction up a value of 92.0% at 1.5 m. Within the topsoil A-horizon, the clay fraction (25.7%) and organic carbon content (1.16%) were significantly higher than in F1 and were responsible for the higher CEC value (13.6 cmol+/kg) under basic pH conditions (8.2). From the topsoil to the subsoil, we observed a classic decrease in TOC contents, which reached levels similar to those observed for F1 at depths over 0.6 m, whereas pH increased up to 8.7 at a depth of 1.00 m. As observed in all soil pits located in the plain area, the soil profiles were affected by severe waterlogging conditions: i) secondary carbonate precipitation structures in soil voids were localised at a depth of 0.32 m; ii) early traces of waterlogged soil were observed at a depth of 0.36 m (oxidation), and an increase was noted for both density and intensity in deeper soil horizons; and iii) iron and manganese concretions appear at a depth of 0.60 m. The roots were abundant up to depths of 0.60 m and remained visible up to 1.60 m. Root development appeared normal and unaffected by the presence of the water table. There were no visible laterization, as observed in F1 (soils description available in Supplementary data).

Despite its sloping conditions, the F3 position presented deep soil conditions. The global soil texture was dominated by silt and clay fractions. From the topsoil to the subsoil, the soil texture became more clayey: from 28.5% at the soil surface to 36% at 1.30 m. Among the three pits, the F3 position had the highest TOC content (1.69%) within the first 0.20 m (plough layer), which decreases markedly for the underlying soil horizon to a stable value around 0.47%, even for the deepest soil horizons. The pH was less basic than measured for the F2 position, whereas the CEC value ranged between 10.8 and 12.7 cmol+/kg. At this location, no waterlogged horizon was described within the first 1.3 m.

Root structures and waterlogging marks in the pits help to understand the water supply of the vine. The F1 soil profile presented clear lateralising root structures with the appearance of waterlogging marks. These pedological features highlight the impact of the water table on vine rooting. Hence, the rising water table during the winter (Fig. 2) reduced the soil investigation by roots. This reduced the amount of water available for the vine. F2 was located 0.4 m below in the plain area (12.8 m a.s.l. for F1 and 12.4 m a.s.l. for F2) and presented waterlogging marks (Table 1 and Supplementary data). However, these marks had a lower intensity, and the presence of carbonate precipitates in horizons up to 1.60 m indicated that the water table does not rise for a long time in these layers. In addition, the root structure was not affected much by the water table. No laterization was observed, as found for the first profile. Thus, the pedological descriptions (Table 1 and Supplementary data) showed that the water supply to vines in these two soil profiles differs, despite their proximity and similar topographical locations.

3.4. Vine available water estimation

The effective maximum rooting depth (*Erd*) and β parameter was determined based on soil profile descriptions (Table 1 and Supplementary data). For F1 and F2, the deeper boundary for root investigations was constrained by the level of the water table during the winter season (Fig. 2). The presence of the water table from mid-January to mid-June is responsible for waterlogged soil features associated with anoxic conditions that induce vine root necrosis. The difference between F1 and F2 includes a deeper level for F1 conditions and a maximum root density depth of 1.25 and 1.60 m, respectively (Table 2). For F3, no limitation of the soil in root investigations was observed, while the soil profile was developed on the *Fronsadais Molasses* geological formation, constitute by unconsolidated sedimentary rocks (Table 1 and Supplementary data). There was no waterlogged horizon at F3 over the entire profile; however, a survey of water table dynamics (Fig. 2) showed that the water table level increased to 2.00 m below the soil surface around the 1st of April. Then, the depth of maximum roots density was defined as 2.00 m (Table 2).

Among the three locations, F1 had the lowest C-AWC value (81 mm, Table 2) in relation to its sandy-dominated soil texture (Table 1), which provides low water content at field capacity (Bruand et al., 2004). This contrasts with the F2 C-AWC value of 150 mm, which is also located in the plain domain, but the texture shows a significant loamy fraction (Table 1). The F3 location presented an intermediate condition, with a C-AWC value of 114 mm owing to its clayey texture (Table 1). When integrating the potential rooting depth in the P-AWC calculation, the F3 location showed the highest value of 253 mm, which was not significantly different from that calculated for the F2 location (246 mm). The F1 location had the lowest AWC, with a P-AWC of 107 mm (Table 2). The estimated values of TTSW (Table 2) were the lowest for the F3 (50 mm) and F1 (57 mm) locations and the highest for F2 (120 mm).

3.5. Wine quality rank map

The wine quality ranks map is presented in Fig. 4, based on quality rankings established by the winemaker. In this ranking, A-quality is the highest. The first comment considers the spatial cover associated with each rank of the same order, which is almost a third of the total area for each quality (A-quality = 2.77 ha; B-quality = 5.73 ha; C-quality = 4.51 ha). The second observation is that the spatial pattern is associated with quality distribution: A-quality was located on the slope system, whereas B- and C-quality were found in the southern plain, where no A-quality was present. When compared with the soil map stratified in three SFUs, one can say that i) A-quality occurred exclusively in SFU-3, ii) SFU-2 was mainly associated with B-quality, and iii) SFU-1 generated both B- and C-quality. For this last SFU, we noted a clear distribution with B-quality located in the northern part of the SFU, whereas C-quality was clearly observed in the southern part.

3.6. From wine quality map to soil properties

All soil analyses were classified into three classes based on the wine quality ranks map. Then, within a quality class, samples were split depending on the sampling depth, namely topsoil (from the soil surface to 0.2 m) and subsoil (from 0.2 m to 0.8 m). All descriptive statistics for quality and soil depth are summarised in Table 3. Among soil properties, soil texture and pH are significant when considering the wine quality categorisation. A-quality was associated with the highest content of both clay and silt fractions under both topsoil and subsoil conditions, whereas sandy fractions were dominant for C-quality regardless of soil depth. A-quality was also strongly correlated with pH status and then $CaCO_3$ content, with the highest values for both pH and $CaCO_3$ measured for this quality class. Stratification was less

Table 2
Calculation of available soil water for the vine at the locations of the three pits (F1, F2 and F3).

Pit	C-AWC [mm]	P-AWC [mm]	TTSW [mm]	Beta [m]	Erd [m]
F1	81	107	57	0.92	*1.25*
F2	150	256	127	*1.05*	*1.60*
F3	114	253	50	*1.50*	*2.00*

pronounced for organic carbon and nitrogen values. A-quality covered both the highest variability and the highest mean value for TOC content in topsoil. For topsoil condition mean value stratification is ranked with wine quality whereby the lowest quality was associated with the lowest mean TOC content. To complement the trends in TOC, total nitrogen was well stratified with the highest nitrogen values measured for the highest quality. The C/N ratios were significantly lower for the highest wine quality. The final comments are for CEC and major elements (Ca, Mg, and K), which are consistently related to the stratification of other soil parameters: CEC values and the concentrations of major elements decrease with decreasing wine quality. We noted that for CEC and CaO, the B-quality presented the largest numerical values. To refine our analysis, specific descriptive statistics were calculated for SFU-1, whereby B- and C-quality were well spatially distributed (Supplementary data). Based on these statistics, no significant difference was found between the main soil parameters when comparing B- and C-quality classes.

4. Discussion

4.1. Water availability

When considering factors controlling red wine quality, the vine water supply is a major parameter. Several studies (Choné et al., 2000; Choné, 2001; Dry and Loveys, 1998; Ojeda et al., 2002; Seguin, 1986; Smart and Robinson, 1991; Tregoat, 2003; Tregoat et al., 2002; Van Leeuwen, 2010; Van Leeuwen et al., 2009) have highlighted the importance of marked water deficit after flowering to promote the synthesis of polyphenols, which are essential to ensure the quality of red wine grapes (Carbonneau, 1986; Matthews and Anderson, 1988; Ojeda et al., 2002; Van Leeuwen and Seguin, 1994). Conversely, excess water stress reduces quality, while blocking photosynthesis reduces polyphenol synthesis (Deloire et al., 2004). For this reason, ideotypes of good soils for qualitative red wine are often presented as those having thin soil volume or with high stoniness and conditions with a limited volume of water available to the vine.

Regardless of the calculation used, the F1 location presented the lowest AWC (Table 2). This was explained by its sandy texture (Table 1), which has a low potential for water retention and capillarity, and the shallow water table at the end of winter, which constrains the rooting depth. The values calculated for the F2 location were consistently high in relation to its loamy soil texture and rooting potential (Tables 1 and 2). The estimated water storage capacity for the F3 location seemed more sensible for use in calculations, while (i) AWC was highly sensible to assess rooting depth conditions then system architecture at a potential investigation depth of 2.00 m (Table 2) and (ii) TTSW calculation integrated the capability of roots to extract water at water potentials different from the theoretical wilting point, after which the quantity of non-available water was associated with high water potential in clayey soils (Bruand et al., 2004).

4.2. Nutrient availability

In contrast to water availability, overall stock and nutrient availability is essential for wine production (White, 2003). Among the critical nutrients, nitrogen forms should be present in sufficient quantities; however, some studies (Tregoat et al., 2002; Van Leeuwen et al., 2000) have shown that a limited supply of nitrogen to the vine may help to improve the quality of red wine. In our study, descriptive statistics (Table 3) showed that the A-horizon of A-quality had an average content of 1.08‰ (±0.41‰ standard deviation), whereas the values decreased with decreasing wine quality: 0.83‰ (±0.33‰ standard deviation) for B-quality and 0.78‰ (±0.35‰ standard deviation) for C-quality. The highest nitrogen content for A-horizons was observed for soils located in the most qualitative field units (Table 3). Although not consistent with the findings of Van Leeuwen et al. (2000), these results converge with comments by Fierer (2017) and Costantini et al. (2015) suggesting that other geochemical and microbiological parameters should be screened and not solely for topsoil horizons. Focusing on

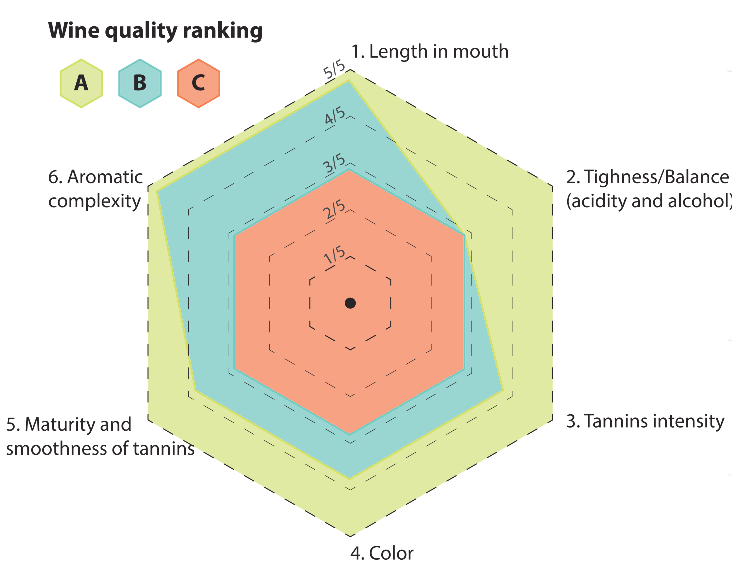

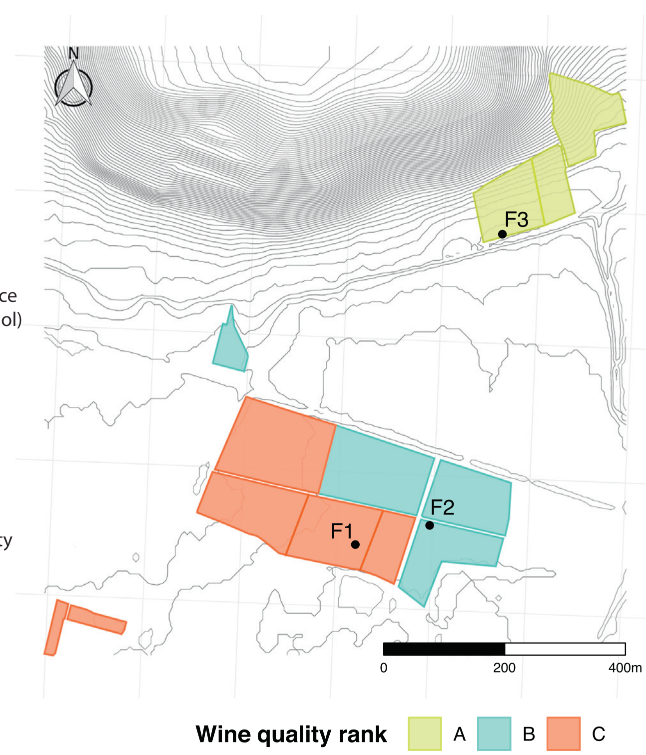

Fig. 4. (a) Wine quality ranking from A (best) to C (worst) and corresponding tasting markers rated from 1 to 5. (1) length in mouth, (2) tightness/balance (acidity and alcohol), (3) tannins intensity, (4) color, (5) maturity and smoothness of tannins, (6) aromatic complexity. (b) Most frequent wine quality rank for each vineyard plot from 2012 to 2018.

Table 3
Descriptive statistics for soil properties for each wine quality area at two different soil depths. Clay(%), Silt(%), Sand(%), TOC(total organic carbon in %), Total N(total nitrogen in ‰), C/N (carbon to nitrogen ratio, without unit), CEC(cation exchange capacity in cmol+/kg), CaO(mg/kg), MgO(mg/kg), K2O(mg/kg), pH H2O(without unit), Total CaCO3(%).

Quality	Average depth	Parameter	Unit	Count	Mean	SD	Min	Q25	Median	Q75	Max
A	(0,20]	Clay	%	19	30.07	5.82	20.40	26.20	29.80	32.65	41.30
		Silt	%	19	35.90	7.07	25.60	30.30	35.20	40.70	49.30
		Sand	%	19	34.02	11.18	10.90	28.15	32.30	42.05	53.50
		TOC	%	19	0.93	0.45	0.35	0.49	0.81	1.34	1.69
		Total N	‰	19	1.08	0.41	0.50	0.70	1.00	1.40	1.90
		C/N		19	8.85	4.01	2.20	7.15	8.30	9.25	23.20
		CEC	cmol+/kg	19	10.38	1.70	7.80	9.00	10.20	11.60	13.90
		CaO	mg/kg	19	10,679.58	870.53	8243.00	10,480.50	10,804.00	11,100.50	11,746.00
		MgO	mg/kg	19	345.32	124.64	153.00	255.50	326.00	407.50	626.00
		K_2O	mg/kg	19	242.95	98.21	114.00	176.00	231.00	293.50	471.00
		pH H_2O		19	8.41	0.21	7.90	8.30	8.40	8.55	8.80
		Total $CaCO_3$	%	19	20.67	7.17	4.00	15.80	20.20	26.50	30.60
	(20,80]	Clay	%	3	24.60	16.91	5.40	18.25	31.10	34.20	37.30
		Silt	%	3	43.97	20.32	21.00	36.15	51.30	55.45	59.60
		Sand	%	3	31.40	37.27	3.00	10.30	17.60	45.60	73.60
		TOC	%	3	0.29	0.12	0.17	0.23	0.29	0.35	0.41
		Total N	‰	3	0.43	0.19	0.27	0.32	0.37	0.50	0.64
		C/N		3	7.23	3.11	4.70	5.50	6.30	8.50	10.70
		CEC	cmol+/kg	3	8.17	4.82	2.60	6.70	10.80	10.95	11.10
		CaO	mg/kg	3	9938.33	1126.19	8638.00	9607.00	10,576.00	10,588.50	10,601.00
		MgO	mg/kg	3	476.00	211.90	272.00	366.50	461.00	578.00	695.00
		K_2O	mg/kg	3	127.67	88.10	59.00	78.00	97.00	162.00	227.00
		pH H_2O		3	8.50	0.26	8.30	8.35	8.40	8.60	8.80
		Total $CaCO_3$	%	3	41.20	7.79	34.40	36.95	39.50	44.60	49.70
B	(0,20]	Clay	%	23	20.73	7.17	8.50	13.60	23.00	26.60	30.90
		Silt	%	23	19.88	8.01	9.20	14.40	15.90	27.35	33.60
		Sand	%	23	59.38	14.39	36.80	44.20	62.20	71.25	82.30
		TOC	%	23	0.90	0.26	0.47	0.73	0.93	1.08	1.63
		Total N	‰	23	0.99	0.32	0.40	0.85	1.00	1.10	2.00
		C/N		23	9.40	1.79	5.80	8.40	9.50	10.55	12.40
		CEC	cmol+/kg	23	9.77	3.19	4.30	7.30	11.30	12.10	13.80
		CaO	mg/kg	23	5421.26	3677.77	936.00	2204.50	4310.00	9249.00	11,049.00
		MgO	mg/kg	23	237.83	83.55	90.00	195.50	244.00	319.50	339.00
		K_2O	mg/kg	23	204.70	85.73	96.00	147.50	169.00	239.00	418.00
		pH H_2O		23	7.76	0.56	6.40	7.50	7.90	8.20	8.40
		Total $CaCO_3$	%	23	2.01	2.41	0.25	0.25	0.25	3.75	7.80
	(20,80]	Clay	%	2	25.45	2.05	24.00	24.73	25.45	26.17	26.90
		Silt	%	2	20.25	7.00	15.30	17.78	20.25	22.72	25.20
		Sand	%	2	54.30	9.05	47.90	51.10	54.30	57.50	60.70
		TOC	%	2	0.44	0.21	0.29	0.36	0.44	0.51	0.58
		Total N	‰	2	0.44	0.19	0.31	0.38	0.44	0.51	0.58
		C/N		2	9.70	0.42	9.40	9.55	9.70	9.85	10.00
		CEC	cmol+/kg	2	10.90	0.85	10.30	10.60	10.90	11.20	11.50
		CaO	mg/kg	2	9703.50	943.99	9036.00	9369.75	9703.50	10,037.25	10,371.00
		MgO	mg/kg	2	351.00	16.97	339.00	345.00	351.00	357.00	363.00
		K_2O	mg/kg	2	78.50	26.16	60.00	69.25	78.50	87.75	97.00
		pH H_2O		2	8.45	0.07	8.40	8.43	8.45	8.47	8.50
		Total $CaCO_3$	%	2	5.95	4.31	2.90	4.42	5.95	7.47	9.00
C	(0,20]	Clay	%	29	8.87	2.41	5.80	7.00	8.10	10.90	14.20
		Silt	%	29	10.11	2.43	5.20	8.00	9.40	12.30	14.50
		Sand	%	29	81.01	4.38	72.80	78.20	82.50	84.90	86.40
		TOC	%	29	0.70	0.34	0.17	0.47	0.64	0.93	1.51
		Total N	‰	29	0.67	0.28	0.20	0.50	0.67	0.90	1.33
		C/N		29	10.12	1.68	7.70	8.70	9.70	11.60	13.10
		CEC	cmol+/kg	29	4.21	1.39	2.00	3.30	3.90	4.70	7.30
		CaO	mg/kg	29	1674.45	1304.03	379.00	830.00	1196.00	1937.00	4945.00
		MgO	mg/kg	29	87.52	33.33	32.00	59.00	88.00	107.00	153.00
		K_2O	mg/kg	29	140.07	54.85	36.00	100.00	137.00	158.00	276.00
		pH H_2O		29	7.03	0.79	5.70	6.40	7.10	7.50	8.40
		Total $CaCO_3$	%	29	0.25	0.00	0.25	0.25	0.25	0.25	0.25
	(20,80]	Clay	%	15	8.51	2.85	3.20	6.80	8.70	9.60	13.30
		Silt	%	15	8.12	1.45	5.90	7.40	7.90	8.85	11.80
		Sand	%	15	83.37	3.42	78.00	81.05	83.60	84.95	89.00
		TOC	%	15	0.23	0.13	0.06	0.17	0.17	0.26	0.47
		Total N	‰	15	0.24	0.09	0.10	0.20	0.20	0.27	0.50
		C/N		15	9.28	3.01	5.80	7.65	8.70	9.50	15.50
		CEC	cmol+/kg	15	2.74	0.67	1.40	2.40	2.70	3.05	4.10
		CaO	mg/kg	15	1294.73	998.08	494.00	800.00	840.00	1242.00	4171.00
		MgO	mg/kg	15	67.27	20.27	30.00	56.00	72.00	80.00	106.00
		K_2O	mg/kg	15	89.60	27.86	52.00	66.50	81.00	113.50	134.00
		pH H_2O		15	7.67	0.36	7.00	7.50	7.60	7.85	8.30
		Total $CaCO_3$	%	15	0.27	0.09	0.25	0.25	0.25	0.25	0.60

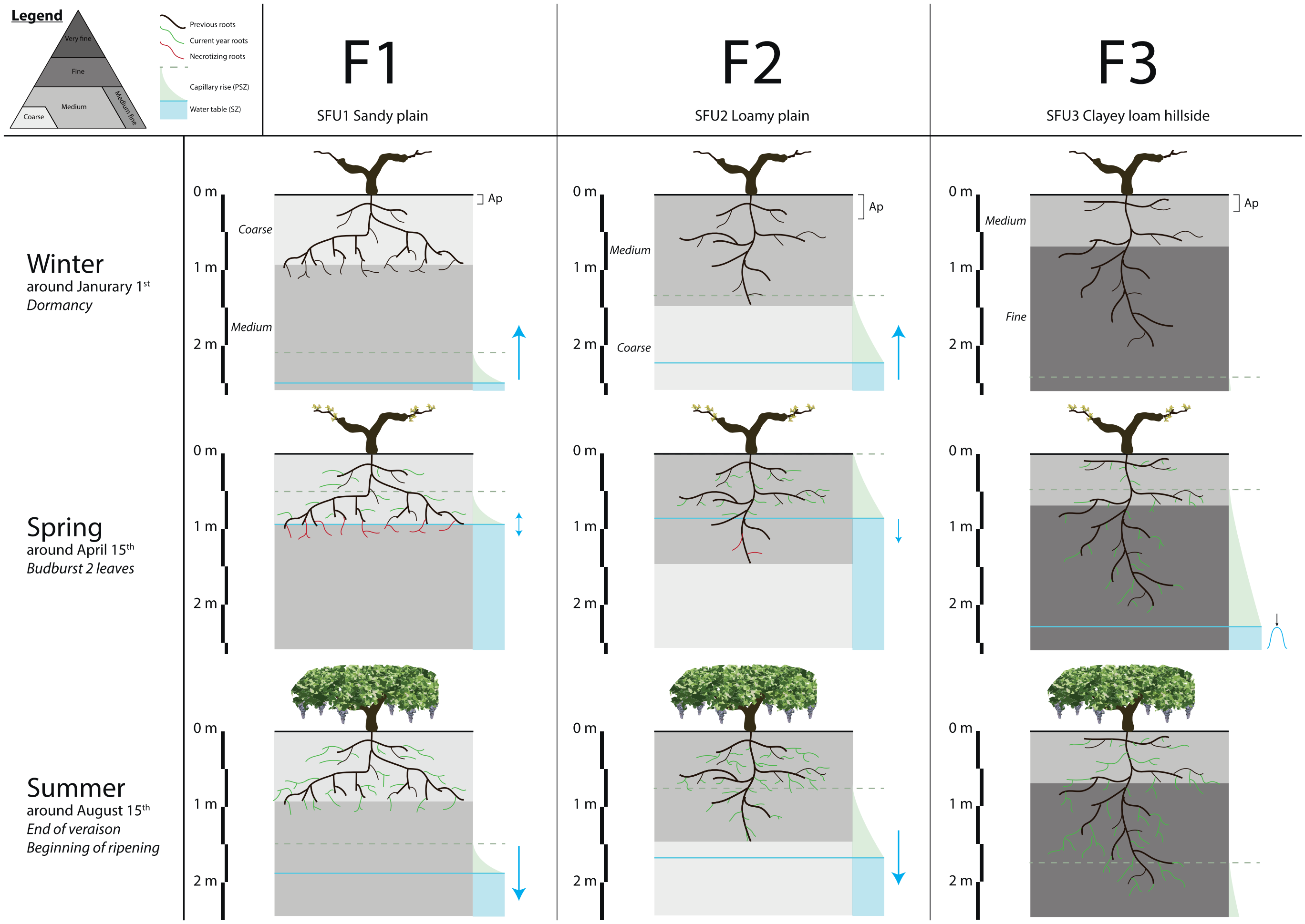

Fig. 5. Conceptual representation of the rooting system of the vine in positions F1–F3 according to the season and water table variations: impact of the saturated zone (SZ) and the partially saturated zone (PSZ).

soil parameters on a pit scale, Table 1 shows that the TOC values and distribution with soil depth differ markedly when comparing pits F1, F2, and F3: (i) TOC contents in the A-horizon increased with increasing wine quality, from 0.41% for F1 to 1.69% for F3, and (ii) a deeper B-horizon for F3 (A-quality) presented TOC content similar to those observed for the A-horizon in F1 (C-quality). This observation of TOC distribution must be coupled with C/N ratio stratification along soil depth. The low C/N ratio (<12) observed for all samples is noteworthy. Similarly, it is notable that F3 (A-quality) presented the highest stock of soil organic carbon and that this stock remained important even for deep B-horizons where the C/N ratio indicated the satisfactory availability of nutrients in relation to the satisfactory potential activity of soil microorganisms. A similar understanding can be reached based on the origin of soil organic matter for B-horizons. Here, observations of the root system during field investigations can be helpful: for F3, field observation revealed the presence of roots down to 1.60 m (the bottom of the pit) and no limitation to root investigation (soils description available in Supplementary data). Notably, regarding water supply, the root system can be used to investigate deep soil horizons, and the associated yearly biomass production of functional roots constituted a large input of fresh organic matter, whose subsequent mineralisation facilitated by the low C/N ratio could serve the nutritional needs. This stratification of soil organic matter in deep soil horizons in relation to root biomass is well established in crop production systems. Furthermore, studies have shown the overall contribution of root biomass to soil organic carbon stocks (Balesdent and Balabane, 1996; Clemmensen et al., 2015; Kuzyakov and Domanski, 2000; Mendez-Millan et al., 2010), and this contribution could be significant for deeper soil horizons (Mendez-Millan et al., 2012; Rasse et al., 2005; Rumpel and Kögel-Knabner, 2011). Finally, CEC can be discussed in relation mainly to both soil texture and soil organic carbon content. The F1 position in C-quality was dominated over the whole soil profile by a sandy fraction (Table 1) and a low TOC content, and subsequently associated with a CEC value lower than 3.6 cmol+/kg within the first 0.9 m (Table 1) whereas rooting depth is limited to 1.25 m. At this position, the low quantity of TOC would not supply nutrients to vines in association with soil organic carbon mineralisation processes, and regardless of the amount of added mineral fertilizers, almost no cation could be adsorbed. Then, for F1, the overall capability of the soil system is extremely low to supply the vine with nutrients. The functioning is clearly different for the F3 location where i) soil texture is dominated by silt and clay fractions, ii) soil organic carbon stock is sufficient to provide the vine with nutrients, and iii) a CEC value of over 10.8 cmol+/kg indicates a reserve of adsorbed cation. In our study, the highest wine quality was observed for soil with a higher potential of supplying the vine with nutrients.

4.3. Soil–vine dynamics

A major soil function is to ensure water and nutrient supplies to the vine (White, 2003). The overall capability of the soil system to meet these needs is part of the complexity met by winegrowers and winemakers when producing high-quality wines. Thus, our main objective was to identify the pedological parameters that may limit or favour parameters associated with quality wine production. First, we performed a soil investigation, which was independent from winegrower and winemaker knowledge. As a result, we produced a high-resolution soil map and distinguished three SFUs (Fig. 3). Then, for each SFU, we characterised the fine soil profile (Table 1 and Supplementary data) and monitored the water table level in order to refine knowledge on soil–water and root–vine interactions. Second, we obtained data from winemakers regarding wine quality in order to produce a spatial representation of it (Fig. 4). Even if substantial differences exist between the SFU and wine quality ranks maps (Figs. 3 and 4), we observed that A-quality is exclusively produced in SFU-3, and C-quality is exclusively produced in SFU-1. Intermediate B-quality is produced both in SFU-2 and a part of SFU-1. This diversity of wine quality observed in SFU-1 suggests that (i) SFU-1 environmental variability is certainly greater than the one we characterised, or (ii) additional environmental factors ought to be included for a better SFU characterization.

Fig. 5 is a conceptual representation of the "soil-water table" system, which constrains vine root architecture and functioning during the growing period and integrates the main findings of the present study. In this representation, the three sub-systems (SFU-1, SFU-2, and SFU-3) and associated system conditions, *e.g.* soil, water-table, and the roots, are represented at three different dates (t_1, t_2, and t_3). For water-saturated levels, we distinguished the saturated zone (SZ), as measured in piezometers, from the partially saturated zone (PSZ) under the control of capillarity rises. In soil systems, the height of the capillary rise depends on the matrix porosity of each soil (Hillel, 1998). In Fig. 5, we suggested that capillary rises were limited by the coarse textures of F1, intermediate in the loamy textures of F2, and important for the silty-clayey textures of F3.

At t_1 (January), the water table level transitions from the minimum (beginning of winter) to maximum (April) levels. Considering the soil and atmosphere temperatures (under 10 °C), the vine plant is dormant, vine root growth is not active, and soil microbiological activity is overall reduced. During this period, if needed, water will be supplied from topsoil water replenished by frequent rainfall, and nutrients will be delivered by soil solution in relation to the CEC saturation. Then, SFU-2 and SFU-3 will have the best access to both water and nutrients.

At t_2 (April), the water table is at the highest level (the lowest distance between soil surface topography and the water table level). Vine buds open and biomass production (roots and shoots) begins. Soil humidity and temperature conditions are favourable for soil microbiological activity. During this period, the overall capability of the vine plant to collect water is related to its root architecture, which is constrained by the water-table. In SFU-1 and SFU-2, roots are subjected to waterlogged conditions, and root system development is limited by the upper level of the saturated area. Additionally, necrosis may occur in the roots previously located in the newly saturated area. For SFU-3, water will be available in the rooting zone in the partially saturated area, without necrosis damaging the roots. For nutrient needs, all positions present satisfactory conditions for both soil organic matter mineralisation and ammonium nitrification by soil microorganisms. However, when considering the initial stock of TOC and volume of the rooting zone, SFU-3 provides the conditions allowing the best access to soil nutrients without the limitations associated with water excess.

At t_3 (August), the level of the water table transitions from the maximum (t_2) to minimum (beginning of winter) levels. Biomass production (vegetative step) is almost complete, and the growth of roots and shoots decreases, grape berries complete ripening, and maturation begins. Air temperature is responsible for the high ET_0, and soil temperature is optimal, but soil humidity is a limiting factor for soil microbiological activity. During this period without significant rainfall and marked reductions in the water-table level, the root system will be used for water supply. Vines in SFU-1, which at t_2 was under water excess conditions, with a limited root system will have to face water-deficit conditions linked to high hydraulic conductivity of sandy soil. Vines of SFU-2 and SFU-3 will be subjected to moderate water constrains in relation to their intermediate silty-clayey conditions, which are favourable for capillarity rises and have high potential for water retention. During rainy years, SFU-2 may suffer no water stress. Among these two positions, SFU-3 will present conditions of high water stress owing to its clayey soil texture and low annual variability.

5. Conclusion

A relationship between vines and soil exists to meet the water and nutrient requirements of the plant. Our main objective was to identify the pedological parameters that may limit or favour parameters of quality wine production. As a result, we produced a high-resolution soil map and distinguished three SFUs, which were close to the wine quality ranks map. Explanatory factors of this concordance reside in soil, water, and root interactions with time. Taken together, these dynamics of soil, water, and root systems are responsible for differentiation of winemaking wine quality. The best wine qualities were observed under conditions with no limitations to root investigations due to a hard rock layer or waterlogged soil conditions. Additionally, the best soil for quality wine is observed under (i) non-severe water-deficit conditions linked to the overall water retention capacity of silty-clayey soil textures and (ii) no limitations of nutrient conditions linked to important soil organic matter stocks and higher CEC even under high-depth mineral soil conditions.

However, this result implies that deep soil–root interactions should be investigated in order to confirm that the best soil for quality wine arises from both non-severe water deficits and non-limited nutrient conditions.

Supplementary data to this article can be found online at https://doi.org/10.1016/j.scitotenv.2019.133718.

Acknowledgements

This work was supported by Antoine Moueix Properties, Montpellier SupAgro and Bordeaux Sciences Agro as part of Etienne Fayolle's CIFRE PhD. The authors would like to thank the team and collaborators of the Château Capet-Guillier for their support. We also thank Stéphanie Jalabert (Bordeaux Sciences Agro, EA4592 G&E) and Christèle Cornier (AgroValo Méditerranée, partnership service, Montpellier SupAgro) for their support. Lastly, the authors would like to thank the three anonymous reviewers for their high valuable comments and suggestions.

References

Allen, R.G., Pereira, L.S., Raes, D., Smith, M., 1998. Crop Evapotranspiration - Guidelines for Computing Crop Water Requirements - FAO Irrigation and Drainage Paper 56 (No. 56). FAO - Food and Agriculture Organization of the United Nations, Rome.

Archer, E., Saayman, D., 2018. Vine Roots. The Institute for Grape and Wine Sciences (IGWS), Stellenbosch.

Baciocco, K.A., Davis, R.E., Jones, G.V., 2014. Climate and Bordeaux wine quality: identifying the key factors that differentiate vintages based on consensus rankings. J. Wine Res. 25, 75–90. https://doi.org/10.1080/09571264.2014.888649.

Balesdent, J., Balabane, M., 1996. Major contribution of roots to soil carbon storage inferred from maize cultivated soils. Soil Biol. Biochem. 28, 1261–1263. https://doi.org/10.1016/0038-0717(96)00112-5.

Bertrand, N., Roux, S., Forey, O., Guinet, M., Wery, J., 2018. Simulating plant water stress dynamics in a wide range of bi-specific agrosystems in a region using the BISWAT model. Eur. J. Agron. 99, 116–128. https://doi.org/10.1016/j.eja.2018.06.001.

Blotevogel, S., Schreck, E., Laplanche, C., Besson, P., Saurin, N., Audry, S., Viers, J., Oliva, Priscia, 2019. Soil chemistry and meteorological conditions influence the elemental profiles of West European wines. Food Chem. 125033 https://doi.org/10/gf3x38.

Bois, B., Van Leeuwen, C., Pieri, P., Gaudillère, J.-P., Saur, E., Joly, D., Wald, L., Grimal, D., 2008. Viticultural agroclimatic cartography and zoning at mesoscale level using terrain information, remotely sensed data and weather station measurements. Case study of Bordeaux winegrowing area. Implications on Vine Development and Fruit Ripening. Université Bordeaux. Presented at the VIIth International Terroir Congress, p. 9 https://doi.org/10.1007/978-94-007-5642-7_6.

Bonfante, A., Basile, A., Langella, G., Manna, P., Terribile, F., 2011. A physically oriented approach to analysis and mapping of terroirs. Geoderma 167–168, 103–117. https://doi.org/10.1016/j.geoderma.2011.08.004.

Bonfante, A., Monaco, E., Langella, G., Mercogliano, P., Bucchignani, E., Manna, P., Terribile, F., 2018. A dynamic viticultural zoning to explore the resilience of terroir concept

under climate change. Sci. Total Environ. 624, 294–308. https://doi.org/10.1016/j.scitotenv.2017.12.035.
Brillante, L., Bois, B., Lévêque, J., Mathieu, O., 2016. Variations in soil-water use by grapevine according to plant water status and soil physical-chemical characteristics—a 3D spatio-temporal analysis. Eur. J. Agron. 77, 122–135. https://doi.org/10.1016/j.eja.2016.04.004.
Bruand, A., Duval, O., Cousin, I., 2004. Estimation des propriétés de rétention en eau des sols à partir de la base de données SOLHYDRO: Une première proposition combinant le type d'horizon, sa densité apparente. Etude et Gestion des Sols 11 (3), 323–334.
Camps, J.O., Ramos, M.C., 2012. Grape harvest and yield responses to inter-annual changes in temperature and precipitation in an area of north-east Spain with a Mediterranean climate. Int. J. Biometeorol. 56, 853–864 https://doi.org/10/cxvhwj.
Carbonneau, A., 1986. Stress modérés sur feuillage induits par le système de conduite et régulation photosynthétique de la vigne. Symp. Physiologie de La Vigne. OIV, Bordeaux, pp. 378–385.
Choné, X., 2001. Contribution à l'étude des terroirs de Bordeaux: étude des déficits hydriques modérés, de l'alimentation en azote et de leurs effets sur le potentiel aromatique des raisins de Vitis vinifera L. cv. Sauvignon blanc (PhD. Thesis). Bordeaux 2).
Choné, X., Dubourdieu, D., Van Leeuwen, C., Tregoat, O., 2000. Déficit hydrique modéré de la vigne: parmi les 3 applications de la chambre à pression, le potentiel tige est l'indicateur le plus précis. Journal international des sciences de la vigne et du vin 34, 169–176.
Clemmensen, K.E., Finlay, R.D., Dahlberg, A., Stenlid, J., Wardle, D.A., Lindahl, B.D., 2015. Carbon sequestration is related to mycorrhizal fungal community shifts during long-term succession in boreal forests. New Phytol. 205, 1525–1536. https://doi.org/10.1111/nph.13208.
Costantini, E.A.C., Bucelli, P., 2014. Soil and Terroir, in: Soil Security for Ecosystem Management. Springer, Cham, Cham, pp. 97–133.
Costantini, E.A.C., Barbetti, R., Fantappiè, M., L'Abate, G., Lorenzetti, R., Magini, S., 2013. Pedodiversity. In: Costantini, E.A.C., Dazzi, C. (Eds.), The Soils of Italy. Springer Netherlands, Dordrecht, pp. 105–178.
Costantini, E.A.C., Agnelli, A.E., Fabiani, A., Gagnarli, E., Mocali, S., Priori, S., Simoni, S., Valboa, G., 2015. Short-term recovery of soil physical, chemical, micro- and mesobiological functions in a new vineyard under organic farming. SOIL 1, 443–457. https://doi.org/10.5194/soil-1-443-2015.
Costantini, E.A.C., Castaldini, M., Diago, M.P., Giffard, B., Lagomarsino, A., Schroers, H.-J., Priori, S., Valboa, G., Agnelli, A.E., Akça, E., D'Avino, L., Fulchin, E., Gagnarli, E., Kiraz, M.E., Knapič, M., Pelengić, R., Pellegrini, S., Perria, R., Puccioni, S., Simoni, S., Tangolar, S., Tardaguila, J., Vignozzi, N., Zombardo, A., 2018. Effects of soil erosion on agro-ecosystem services and soil functions: a multidisciplinary study in nineteen organically farmed European and Turkish vineyards. J. Environ. Manag. 223, 614–624 https://doi.org/10/gd5d9q.
de Andrés-de Prado, R., Yuste-Rojas, M., Sort, X., Andrés-Lacueva, C., Torres, M., Lamuela-Raventós, R.M., 2007. Effect of soil type on wines produced from Vitis vinifera L. Cv. Grenache in commercial vineyards. J. Agric. Food Chem. 55, 779–786. https://doi.org/10.1021/jf062446q.
Deloire, A., Carbonneau, A., Wang, Z., Ojeda, H., 2004. Vine and Water: A Short Review. 1 38. , pp. 1–13 https://doi.org/10.20870/oeno-one.2004.38.1.932.
Deloire, A., Vaudour, E., Carey, V.A., Bonnardot, V., Van Leeuwen, C., 2005. Grapevine Responses to Terroir: A Global Approach. 1 39. , pp. 149–162 https://doi.org/10.20870/oeno-one.2005.39.4.888.
Dry, P.R., 2016. Understanding the components of terroir. Proceedings of the 16th Australian Wine Industry Technical Conference: Adelaide, South Australia, 24–28 July. The Australian Wine Industry Technical Conference Inc., Glen Osmond, SA, pp. 39–44.
Dry, P.R., Loveys, B.R., 1998. Factors influencing grapevine vigour and the potential for control with partial rootzone drying. Aust. J. Grape Wine Res. 4, 140–148. https://doi.org/10.1111/j.1755-0238.1998.tb00143.x.
Dubreuilh, J., 1995. Carte géologique n°804, Libourne.
Fierer, N., 2017. Embracing the unknown: disentangling the complexities of the soil microbiome. Nat. Rev. Microbiol. 15, 579–590 https://doi.org/10/gbsc5b.
Garcia, M., Ibrahim, H., Gallego, P., Puig, P.H., 2001. Effect of three rootstocks on grapevine (Vitis vinifera L.) cv. Negrette, grown hydroponically. II. Acidity of musts and wines. South African Journal of Enology and Viticulture 22, 104–106. https://doi.org/10.21548/22-2-2203.
Garcia, L., Celette, F., Gary, C., Ripoche, A., Valdés-Gómez, H., Metay, A., 2018. Management of service crops for the provision of ecosystem services in vineyards: a review. Agric. Ecosyst. Environ. 251, 158–170. https://doi.org/10.1016/j.agee.2017.09.030.
Hannah, L., Roehrdanz, P.R., Ikegami, M., Shepard, A.V., Shaw, M.R., Tabor, G., Zhi, L., Marquet, P.A., Hijmans, R.J., 2013. Climate change, wine, and conservation. Proc. Natl. Acad. Sci. 110, 6907–6912 https://doi.org/10/k5f.
Hillel, D., 1998. Environmental Soil Physics: Fundamentals, Applications, and Environmental Considerations. Academic Press. ed, Elsevier.
Huglin, P., 1978. Nouveau mode d'évaluation des possibilités héliothermiques d'un milieu viticole. Comptes rendus des seances.
IPCC, 2014. Climate Change 2014: Synthesis Report. Contribution of Working Groups I, II and III to the Fifth Assessment Report of the Intergovernmental Panel on Climate Change. vol. 169.
IUSS Working Group WRB, 2015. World Reference Base for Soil Resources 2014, Update 2015: International Soil Classification System for Naming Soils and Creating Legends for Soil Maps (World Soil Resources Reports No. 106). FAO, Rome.
Jahn, R., Blume, H.P., Asio, V.B., Spaargaren, O., Schad, P., 2006. Guidelines for soil description. 4th ed. ed. Food and Agriculture Organization of the United Nations, Rome.
Jones, G.V., Davis, R.E., 2000. Climate Influences on Grapevine Phenology, Grape Composition, and Wine Production and Quality for Bordeaux, France. vol. 51 p. 14.
Kodur, S., 2011. Effects of juice pH and potassium on juice and wine quality, and regulation of potassium in grapevines through rootstocks (Vitis): a short review. VITIS Journal of Grapevine Research 50, 1–6.
Kuzyakov, Y., Domanski, G., 2000. Carbon input by plants into the soil. Review. J. Plant Nutr. Soil Sci. 163, 421–431. https://doi.org/10.1002/1522-2624(200008)163:4<421::AID-JPLN421>3.0.CO;2-R.
Lacape, M.J., Wery, J., Annerose, D.J.M., 1998. Relationships Between Plant and Soil Water Status in Five Field-grown Cotton žGossypium Hirsutum L./Cultivars. vol. 15.
Mackenzie, D.E., Christy, A.G., 2005. The role of soil chemistry in wine grape quality and sustainable soil management in vineyards. Water Sci. Technol. 51, 27–37. https://doi.org/10.2166/wst.2005.0004.
Maltman, A., 2008. The role of vineyard geology in wine typicity. J. Wine Res. 19, 1–17. https://doi.org/10.1080/09571260802163998.
Marciniak, M., Reynolds, A.G., Brown, R., 2013. Influence of water status on sensory profiles of Ontario Riesling wines. Food Res. Int. 54, 881–891. https://doi.org/10.1016/j.foodres.2013.08.030.
Matthews, M.A., 2016. Terroir and Other Myths of Winegrowing. Univ of California Press.
Matthews, M.A., Anderson, M.M., 1988. Fruit ripening in Vitis vinifera L.: responses to seasonal water deficits. Am. J. Enol. Vitic. 39, 313–320.
Mendez-Millan, M., Dignac, M.-F., Rumpel, C., Rasse, D.P., Derenne, S., 2010. Molecular dynamics of shoot vs. root biomarkers in an agricultural soil estimated by natural abundance 13C labelling. Soil Biol. Biochem. 42, 169–177. https://doi.org/10.1016/j.soilbio.2009.10.010.
Mendez-Millan, M., Dignac, M.-F., Rumpel, C., Rasse, D.P., Bardoux, G., Derenne, S., 2012. Contribution of maize root derived C to soil organic carbon throughout an agricultural soil profile assessed by compound specific 13C analysis. Organic Geochemistry, Organic Isotopes in Soil 42, 1502–1511. https://doi.org/10.1016/j.orggeochem.2011.02.008.
Ministère de l'Agriculture et de l'Alimentation, 2017a. Cahier des charges de l'appellation d'origine contrôlée « SAINT-EMILION ».
Ministère de l'Agriculture et de l'Alimentation, 2017b. Cahier des charges de l'appellation d'origine contrôlée « SAINT-EMILION GRAND CRU ».
Morlat, R., Bodin, F., 2006. Characterization of viticultural terroirs using a simple field model based on soil depth – II. Validation of the grape yield and berry quality in the Anjou vineyard (France). Plant Soil 281, 55–69. https://doi.org/10.1007/s11104-005-3769-z.
Ojeda, H., Andary, C., Kraeva, E., Carbonneau, A., Deloire, A., 2002. Influence of pre- and postveraison water deficit on synthesis and concentration of skin phenolic compounds during berry growth of Vitis vinifera cv. Shiraz. Am. J. Enol. Vitic. 53, 261–267.
Peel, M.C., Finlayson, B.L., McMahon, T.A., 2007. Updated world map of the Köppen-Geiger climate classification. Hydrol. Earth Syst. Sci. 11, 1633–1644. https://doi.org/10.5194/hess-11-1633-2007.
Pellegrino, A., Lebon, E., Voltz, M., Wery, J., 2004. Relationships between plant and soil water status in vine (Vitis vinifera L.). Plant Soil 266, 129–142. https://doi.org/10.1007/s11104-005-0874-y.
Penman, H.L., 1948. Natural evaporation from open water, bare soil and grass. Proceedings of the Royal Society of London. Series A, Mathematical and Physical Sciences 193, 120–145 https://doi.org/10/dcq8mv.
Priori, S., Pellegrini, S., Perria, R., Puccioni, S., Storchi, P., Valboa, G., Costantini, E.A.C., 2019. Scale effect of terroir under three contrasting vintages in the Chianti Classico area (Tuscany, Italy). Geoderma 334, 99–112. https://doi.org/10.1016/j.geoderma.2018.07.048.
QGIS Development Team, 2019. QGIS Geographic Information System. Open Source Geospatial Foundation Project.
R Core Team, 2014. R: A Language and Environment for Statistical Computing. R Foundation for Statistical Computing, Vienna, Austria.
Rasse, D.P., Rumpel, C., Dignac, M.-F., 2005. Is soil carbon mostly root carbon? Mechanisms for a specific stabilisation. Plant Soil 269, 341–356. https://doi.org/10.1007/s11104-004-0907-y.
Ratliff, L.F., Ritchie, J.T., Cassel, D.K., 1983. Field-measured limits of soil water availability as related to laboratory-measured properties. Soil Sci. Soc. Am. J. 47, 770–775. https://doi.org/10.2136/sssaj1983.03615995004700040032x.
Retallack, G.J., Burns, S.F., 2016. The effects of soil on the taste of wine. GSA Today 26. https://doi.org/10.1130/GSATG260A.1.
Rodrigo-Comino, J., 2018. Five decades of soil erosion research in "terroir". The state-of-the-art. Earth Sci. Rev. 179, 436–447. https://doi.org/10.1016/j.earscirev.2018.02.014.
Rumpel, C., Kögel-Knabner, I., 2011. Deep soil organic matter—a key but poorly understood component of terrestrial C cycle. Plant Soil 338, 143–158. https://doi.org/10.1007/s11104-010-0391-5.
Seguin, G., 1986. Terroirs and pedology of wine growing. Experientia 42, 861–873. https://doi.org/10.1007/BF01941763.
Smart, R., Robinson, M., 1991. Sunlight Into Wine. A Handbook for Winegrape Canopy Management. Winetitles, Adelaide.
Tonietto, J., Carbonneau, A., 2004. A multicriteria climatic classification system for grape-growing regions worldwide. Agric. For. Meteorol. 124, 81–97. https://doi.org/10.1016/j.agrformet.2003.06.001.
Tregoat, O., 2003. Caractérisation du régime hydrique et du statut azoté de la vigne par des indicateurs physiologiques dans une étude terroir au sein de huit grands crus de Bordeaux : Influence sur le comportement de la vigne et la maturation du raisin (PhD. Thesis). Bordeaux 2, Bordeaux).
Tregoat, O., Van Leeuwen, C., Choné, X., Gaudillère, J.-P., 2002. Etude du régime hydrique et de la nutrition azotée de la vigne par des indicateurs physiologiques. J. Int. Sci. Vigne Vin 36, 133–142.
Van Leeuwen, C., 1989. Carte des sols du vignoble de Saint-Emilion.
Van Leeuwen, C., 2010. Terroir: the effect of the physical environment on vine growth, grape ripening and wine sensory attributes. Managing Wine Quality. Elsevier, pp. 273–315.

Van Leeuwen, C., Seguin, G., 1994. Incidence de l'alimentation en eau de la vigne, appreciee par l'etat hydrique du feuillage, sur le developpement de l'appareil vegetatif et la maturation du raisin (*Vitis vinifera* variété Cabernet franc, Saint-Emilion 1990). 1 28. , pp. 81–110 https://doi.org/10.20870/oeno-one.1994.28.2.1152.
Van Leeuwen, C., Choné, X., Friant, P., Molot, C.H., Soyer, J.P., Dubourdieu, D., 2000. L'intéret du dosage de l'azote total et de l'azote assimilable dans le moût comme indicateur de la nutrition azotée de la vigne. Journal international des sciences de la vigne et du vin= International journal of vine and wine sciences 34, 75–82.
Van Leeuwen, C., Friant, P., Chone, X., Tregoat, O., Koundouras, S., Dubourdieu, D., 2004. Influence of climate, soil, and cultivar on terroir. Am. J. Enol. Vitic. 55, 207–217.
Van Leeuwen, C., Tregoat, O., Choné, X., Bois, B., Pernet, D., Gaudillère, J.-P., 2009. Vine water status is a key factor in grape ripening and vintage quality for red Bordeaux wine. How can it be assessed for vineyard management purposes. J. Int. Sci. Vigne Vin 43, 121–134.
Vaudour, E., 2002. The quality of grapes and wine in relation to geography: notions of terroir at various scales. J. Wine Res. 13, 117–141. https://doi.org/10.1080/0957126022000017981.
White, R.E., 2003. Soils for Fine Wines. Oxford University Press, Oxford, New York.
Winkler, A.J., Cook, J.A., Kliewer, W.M., Lider, L.A., 1974. General Viticulture: Second Revised Edition. University of California Press.